Real-Time Diagnosing Polymer Processing in Injection Molding Using Ultrasound

Lijuan Zhao,[1] Yu Lai,[1] Chen Pei,[1] Cheng-Kui Jen,[2] Kuo-Ding Wu[2]

[1]*College of Chemistry and Material Science, Sichuan Normal University, Chengdu 610068, China*
[2]*Industrial Materials Institute, National Research Council Canada, Boucherville, Quebec J4B 6Y4, Canada*

Received 22 February 2011; accepted 5 January 2012
DOI 10.1002/app.36868
Published online in Wiley Online Library (wileyonlinelibrary.com).

ABSTRACT: Ultrasonic diagnosing technique with a new high-temperature ultrasonic transducer is developed to real-time diagnose polymer processing and its morphology changes in injection molding processing. Compared with the previous researches, the new technique can provide more and accurate information. In this study, ultrasound diagnosis shows that longitudinal wave can real-time characterize the data of the injection process and polymer morphology changes, including melt flow arrival time, the part ejection time, filling and packing stages, polymer solidification process, and the morphology changes during polymer crystallization. Shear waves can real-time diagnose Young's and shear storage modulus, anisotropy property of polymer in injection molding. During our research, real-time ultrasonic diagnosis shows that the storage modulus along the vertical direction is larger than that of the parallel to the melt flow direction under our setup injection conditions. Scanning electron microscopy and dynamic mechanical analysis measurements present that it is because the crystalline lamellas of HDPE are parallel arrangement and grow in a vertical to melt flow direction owing to injection shear force under a certain injection conditions. © 2012 Wiley Periodicals, Inc. J Appl Polym Sci 000: 000–000, 2012

Key words: ultrasound; real-time; injection molding; processing; polymer storage modulus

INTRODUCTION

Injection molding (IM) is one of the most versatile and important processing methods and it is capable of mass-producing complicated plastic parts with excellent dimensional tolerance. More than 33% of all polymeric material processing use this technique.[1] As we know, polymer material properties, including their rheological behavior, mechanical and transport properties, will undergo complicated thermomechanical histories and experience significant changes owing to large pressure variations and rapid cooling during IM. However, injection machine is like a sealed box during the whole process and polymers are manufactured inside it before molded parts are ejected. The morphology and structure of final polymer parts are controlled by machine variables and process variables which are setup in advance.[2–4] In fact, the inherent and nonuniform material properties are further affected by mold cooling, packing, constraints of mold geometry, and the possible presence of reinforcing fibers. As a result, the morphology and structure of the final injection-molded product are inherently not easy to be predicted or controlled as we expect. Nowadays, as plastics applications are growing and developing, how to meet the part quality of customer demands is crucial to the survival and success of enterprises.[5] Hence, IM process has been an active research area for many years, as part quality and yield requirements become more stringent.[6–9]

The pressure and temperature sensors, which are exerted into the mold walls, are currently well known to be used in commercial molding systems for controlling between injection phases and packing phase and for Statistical Process Control.[10,11] Obviously, the drawbacks of these sensors are primarily the invasive nature in measurement, for these techniques require holes to cut into the mold. Several research groups have responded this problem by investigating ultrasonic techniques, owing to its noninvasive, simplicity, rapid speed, portability, safety, and capability to probe the interior of an opaque material. Piche et al. at the National Research Council in Canada have performed a lot of interesting and meaningful works using ultrasonic sensors in extrusion, IM, and also as a postmanufacture crystallinity sensor.[12–15] Brown and Coats have used ultrasonic techniques to monitor polymer conditions during extrusion and IM as well.[14,16] Edwards and Thomas have demonstrated a number of techniques to detect molding flaws and monitor molding conditions during IM.[17]

Correspondence to: L. Zhao (lijuan-zhao@sicnu.edu.cn).
Contract grant sponsor: Science and Technology Department of Sichuan Province; contract grant number: 2010JY0123.
Contract grant sponsor: The Science Foundation of Chinapostdoctor.

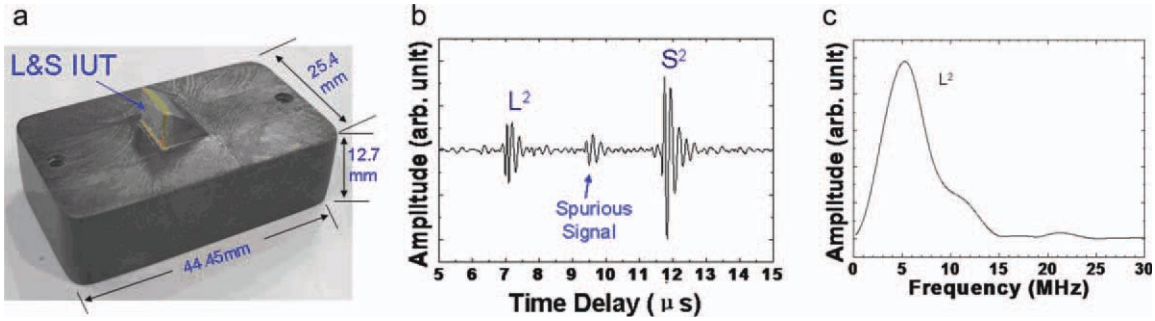

Figure 1 (a) *L–S* probe, (b) ultrasonic *L* and *S* wave signal in time domain of the (a) reflected from the bottom of the probe at room temperature, (c) frequency spectrum of the L^2 echo. [Color figure can be viewed in the online issue, which is available at wileyonlinelibrary.com.]

He et al. have tried to investigate molecular orientation during IM considering different types of polymer, mold geometry, and processing conditions using a normal incidence shear wave ultrasonic sensor.[17,18] They found that the shear wave could travel in different velocities with respect to the particle displacement in different directions. They inferred that the velocity with particle displacement parallel to orientation direction was higher than that of vertical to orientation direction for oriented polymer parts, and the difference in velocity indicated that polymer had different degrees of orientation in its morphology. However, because of high temperature, high pressure, and the very short solidification time in IM, there still remains a challenge task for the detection of technique during IM. Hence, a high-temperature ultrasonic transducer (HTUT), which has large frequency bandwidth, strong signal, and high signal-to-noise, is demanded to investigate polymer processing in IM. However, real-time diagnosis in IM, especially for ultrasound technique, needs to be studied further to get more information during processing and realizes its applications in industrial on a large scale.

In this study, new HTUT probes,[19–21] which could provide simultaneous measurements of one longitudinal wave (*L*), one vertically polarized shear wave ($S_\perp$), and one horizontally polarized shear wave ($S_{||}$), were developed in IM. Besides injection and packing process could be diagnosed, additional information, such as shear and Young's storage modulus and anisotropy of the parts could be obtained real time using the new HTUT probes. Scanning electron microscopy (SEM) and dynamic mechanical analysis (DMA) measurements were carried out to prove the results diagnosed by ultrasonic probes about polymer storage modulus.

EXPERIMENTAL

Materials

High-density polyethylene (HDPE, DMDA-8907) with a melt flow index of 6.75 g/10 min was kindly provided from Dow Chemical (Canada).

Experimental techniques

Ultrasonic probes for polymer IM

Recently, integrated ultrasonic transducers (IUTs) have been made using the sol–gel-based fabrication process. Such IUTs have been operated with a center frequency ranging from 4 to 30 MHz. Their ultrasonic signal strength and bandwidth are comparable to those of the commercially available broadband ultrasonic transducers; however, IUTs which are made in our group can be used at high temperatures (HTUTs) as well.[22] In this study, new HTUTs designed using mode conversion theory will be developed and may provide simultaneous measurements of *L*, $S_\perp$, and $S_{||}$ waves. The design principle and fabrication process of the ultrasonic probe head have been reported in our previous articles.[20,23] Figure 1(a) shows the newly developed HTUT of *L–S* probe for real-time noninvasive monitoring polymer changes in IM process at high temperatures. The simultaneous signals of L^2 and S^2 which are the first round-trip echoes reflected from the bottom of the probe shown in Figure 1(a) are presented in Figure 1(b). The center frequency of the probe's L^2 is about 5 MHz, which is shown in Figure 1(c). The developed $L–S_\perp–S_{||}$ probe is shown in Figure 2(a), with a probe head designed to generate and receive *L*, $S_\perp$, and $S_{||}$ waves simultaneously. Figures 2(b,c) show the ultrasonic signals of L^2, $S_\perp{}^2$, and $S_{||}{}^2$ waves which are the first round-trip echoes reflected from the bottom of the probe at room temperature.

Experiment equipments consisted of HTUTS and IM

In Figure 3(a), four sensor inserts (two *L* probes named UT1 and UT4, two $L–S_\perp–S_{||}$ probes named UT2 andUT3) are fitted into a mold insert with electrical connections, which also demonstrates that sensor array configuration is feasible. The mold, mold insert, and sensor inserts are made of steel. A hole at the center of the mold insert is for a part ejection pin. By replacing the mold insert, the shape and

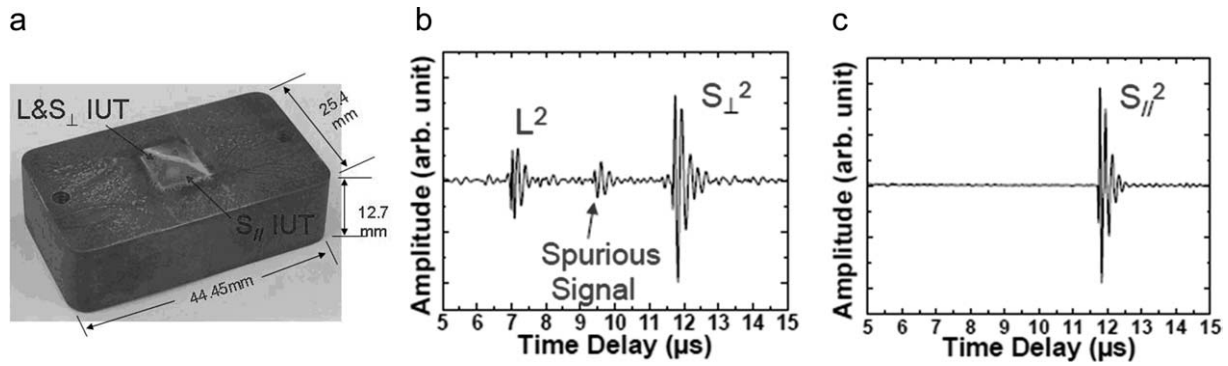

Figure 2 (a) L–$S_{\perp}$–$S_{||}$ probe, (b) ultrasonic signal in time domain of the L^2 and $S_{\perp}{}^2$, (c) and $S_{||}{}^2$ wave of the probe shown in (a) reflected from the bottom of the probe at room temperature. [Color figure can be viewed in the online issue, which is available at wileyonlinelibrary.com.]

dimensions of the molded part can be easily modified to meet the customer's demands. Image of a molded sample part in IM is shown in Figure 3(b), and a rectangular part with dimensions of 76-mm width, 165-mm length, and 1-mm thickness can be molded for the study. The mold insert is then integrated into the mobile mold of a 150 ton Engel IM machine without affecting polymer process in polymer processing as shown in Figure 3(c). Figure 4 shows a cross-sectional view of the mold (mobile and immobile), mold inserts, and molded parts (polymer) with four HTUT sensor inserts (UT1-4). Polymer melt is then injected into the cavity of the mold through the gate at the center of the immobile mold. For comparison purpose with ultrasonic data, a Kistler temperature and cavity pressure sensor, whose sensing end has circular shape with a diameter of 4 mm, are attached to the immobile mold. This Kistler sensor probing end is facing to the UT1 as shown in Figure 4. L^n ($n = 1, 2, 3\ldots$) represents n-th round-trip echoes propagating in the HTUT insert and reflected at the insert–polymer interface and L_{2n} ($n = 1, 2, 3\ldots$) represents those in the polymer and reflected at the polymer–immobile mold interface.

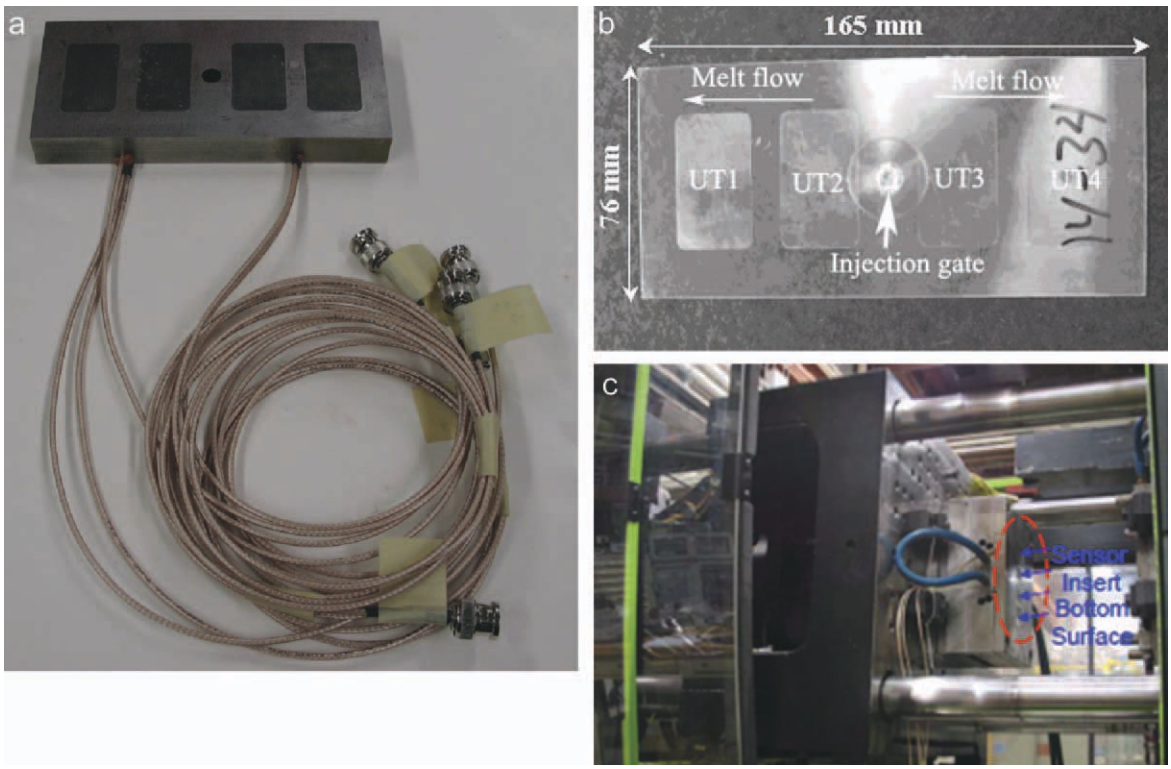

Figure 3 (a) HTUT sensor inserts with an electrical connection embedded in the mold insert used for monitoring injection molding process, (b) image of a molded sample part in IM, (c) mold insert integrated into an IM machine. [Color figure can be viewed in the online issue, which is available at wileyonlinelibrary.com.]

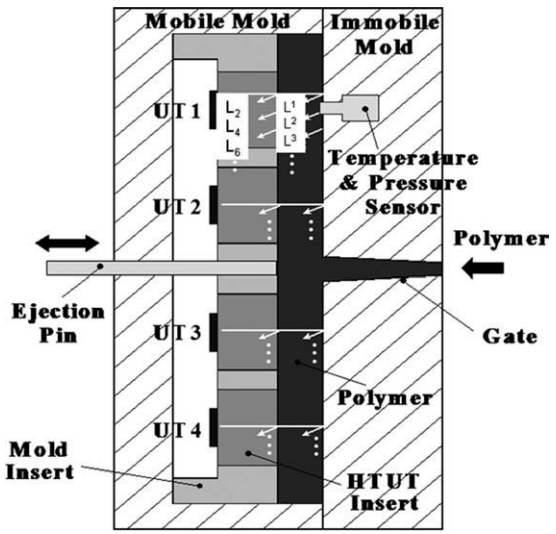

Figure 4 Cross-sectional view of the mold (mobile and immobile), mold insert, and molded part (polymer) with four HTUT sensor inserts (UT1-4). L^n and L_{2n} (n = 1,2,3,...) represent n-th round trip echoes propagating in the HTUT insert and those in the polymer, respectively.

Sample preparation

Using the experiment equipments consisting with HTUTS and injection machine, different samples are prepared under the injection conditions as listed in Table I.

Measurements and characterization

Microscopic Examination

To verify ultrasonic diagnosing results, the samples are needed to be quenched in liquid nitrogen and cryogenically ruptured to get rid of the skin layer of injection samples and then eroded the amorphous phrase using the erodent solvent. The solvent used for surface erosion was the mixed solution of potassium permanganate and concentrated sulfuric acid. The morphology of HDPE was investigated by a JSM-6700F scanning electron microscopy (SEM, JEOL, Japan), which was sputter coated with Au before SEM observations.

Dynamic mechanical analysis

The storage modulus of HDPE samples was tested by DMA (TA instrument, Q-800) using film tensile mode from −20 to 70°C. In measurement, the storage modulus of vertical and parallel to the flow directions was selected on the purpose to see their distinctions, which was also to prove the results of real-time ultrasonic diagnosis.

TABLE I
Typical Molding Conditions for IM[a]

Samples	Injection conditions (mm/s)	Thickness (mm)
HDPE 8907 (210°C)	60	0.8742
HDPE 8907 (220°C)	60	0.864
HDPE 8907 (220°C)	90	0.8672

[a] *Note*: Holding pressure, 60 MPa; cycle time, 30 s; mold temperature, 20°C.

RESULTS AND DISCUSSIONS

Ultrasonic measurements

Figure 5 shows the typical results of acquired signals with the integrated mold insert probe (HTUT) shown in Figure 2(a) during the IM process of a HDPE part at 220°C with a injection speed of 60 mm/s. L^2 is the echo signal reflected at the insert/polymer or air interfaces depending on whether the polymer melt exists at the probe location or not. This L^2 echo signal can be obtained regardless of the thickness of the melt. As shown in Figure 5, once polymer is injected into mold cavity through injection nozzle, ultrasonic signals will penetrate into the polymer and the ultrasonic amplitude will change. The amplitude of L^2 dropping between points A and B is because part of the ultrasound energy propagates to polymer melt after point A, and no ultrasound energy can propagate to polymer after the molded part is ejected at point B. Hence, the time at points of A and B can represent the moment of the melt flow front arrival and the part ejection at the probe location, respectively, which also presents the injection process. When the HDPE melt arrives at the probe location at A, the L_2 echo signal having propagated a round trip through the thickness of the HDPE melt within the mold cavity of 1 mm thickness starts to appear because the probe operates in a pulse/echo mode. At the beginning in injection process, when the melt contacts the cold mold internal surface, its temperature goes down quickly and then the melt starts to solidify. As HDPE is a semi-

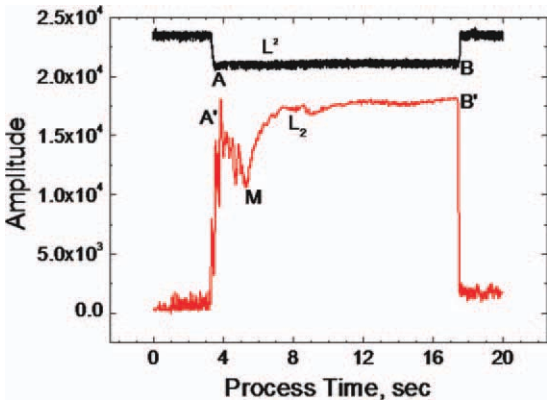

Figure 5 Amplitude variation of L^2 and L_2 measured during injection cycles for HDPE with injection speed of 60 mm/s at 220°C. [Color figure can be viewed in the online issue, which is available at wileyonlinelibrary.com.]

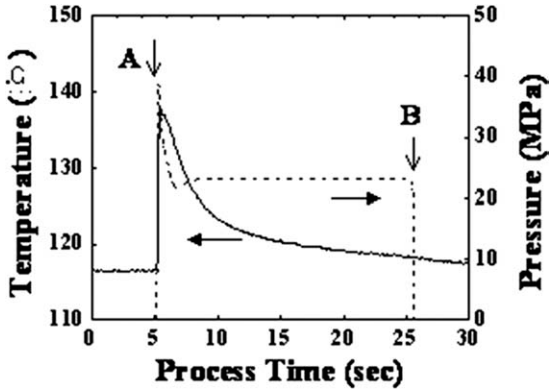

Figure 6 Temperature (solid line) and pressure (dotted line) variation measured with Kistler sensor during IM process. Arrows *A* and *B* indicate the time for flow front arrival at UT1 location, mold opening, respectively.[24]

crystalline polymer, the attenuation will reach a peak which causes a dip in the profile of L_2.[14] This dip is indicated at point of *M* as shown in Figure 5. During the beginning of the IM, the cavity pressure also changes because of the plunger movement, which has been reported earlier[24] and shown in Figure 6. As mentioned above, with process time going, the amplitude of L^2 becomes decreased not only because part of the ultrasound energy propagates into polymer, but also because some of ultrasound energy attenuates owing to the scattering of solid and crystal of HDPE during polymer solidification after it is injected into mold. Hence, it is the filling stage in IM from *A* (*A*′) to *M*, and it is cooling packing stage from *M* to *B*. After point *B*, both L^2 and L_2 move to the original values, which mean that one period of the injection process is over. As shown in Figures 5 and 6, we can see that the changes of ultrasonic amplitude during IM can be used to characterize the period of injection filling, packing, solidification, and the morphological changes of polymer materials. Although pressure and temperature can be used to describe the process of IM, they are less sensitive to the injection process and morphological changes compared with ultrasonic parameters.[18]

The measured time of flights (TOFs) in polymer melt of the *L* and *S* waves are shown in Figure 7 after the cavity pressure becomes steady near the timing T_P which is shown in Figure 7. The TOFs of both *L* and *S* waves decrease owing to the solidification of the melt in the mold cavity in which the *L* and *S* wave velocities increase. As the attenuation of *S* wave is higher in the melt, its TOF can be observed only when the melt solidifies into a viscous condition in which *S* wave probe has enough sensitivity to detect the round trip echo within the melt as indicated as T_S in Figure 7. Assuming the density of the HDPE during the period between T_S and T_B to be 0.94 g/cm^3, the online measured Young's and shear modulus are shown in Figure 8. Hence, ultrasonic diagnosing can be used to real-time assume polymer modulus.

Ultrasonic parameters in detecting HDPE processes will change under different injection conditions as summarized in Table II. As summarized in Table II we can see that longitude velocity increases under higher temperature and higher injection speed, which is owing to different morphologies in HDPE under different injection conditions. The parameter changes of shear waves will be discussed in next part.

Real-time measurements of polymer properties and morphology using ultrasonic technology

The speed of shear wave velocity depends on the stiffness of matrix. As far as an oriented sample with different moduli is concerned, the shear

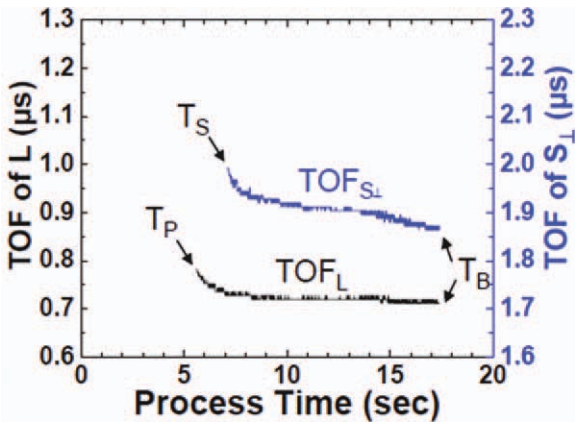

Figure 7 TOF of the measured *L* and $S_\perp$ (Arrow *B* indicates the time for mold opening at probe location). [Color figure can be viewed in the online issue, which is available at wileyonlinelibrary.com.]

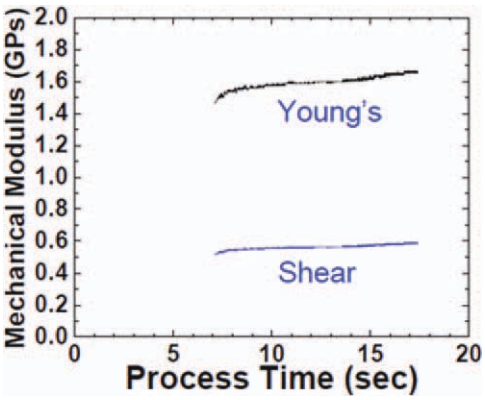

Figure 8 Mechanical modulus of HDPE of the measured *L* and *S* waves in real-time injection molding process. [Color figure can be viewed in the online issue, which is available at wileyonlinelibrary.com.]

TABLE II
Ultrasonic Parameters of HDPE in Different Injection Conditions

Injection conditions	Thickness (mm)	Longitude time delay (μs) (in mold)	Longitude velocity (m/s) (in mold)
210°C (60 mm/s)	0.8742	0.708	2469
220°C (60 mm/s)	0.836	0.676	2473
220°C (90 mm/s)	0.8672	0.700	2477

TABLE III
Real-Time Shear Wave Parameters of HDPE in Different Injection Conditions

Injection conditions	Thickness (mm)	t_H (μs)	t_V (μs)	Δt (μs)
210°C (60 mm/s)	0.8742	2.736	2.08	0.656
220°C (60 mm/s)	0.836	2.425	1.872	0.553
220°C (90 mm/s)	0.8672	2.744	2.008	0.736

stiffness is different. Taking an IM sample as an example, which is shown in Figure 9, because of distinct storage moduli between parallel and vertical to melt flow in IM, there is speed difference when shear wave travels in two ways which can be used to characterize anisotropic distinctions. Generally, the higher the storage modulus, the greater the difference in the shear stiffness is. Consequently, the velocity difference between the speeds of parallel (V_H) and vertical to the melt flow direction (V_V) is much higher. Therefore, the velocity difference ($V_H - V_V$) can be utilized to characterize the degree of polymer property difference. As the corresponding time delay is more convenient than velocity to illuminate the storage modulus, the difference in time delay $\Delta t = (t_V - t_H)$ can be substituted for $\Delta V = (V_H - V_V)$ to characterize the degree of anisotropy. In this article, higher temperature and injection speed are set up in IM to obtain high property difference of crystalline HDPE. When the ultrasound propagates in anisotropic media (uniaxial orientation), shear wave has two characteristic velocities, depending on the direction of the particle displacement vector. According to the property that ultrasound travels in different velocities in anisotropic media, the propagation velocities of our ultrasonic probe which can emit two vertical shear waves simultaneously in this technique are used to detect anisotropic behaviors of the mechanical properties during process. When the particle displacement is in the x direction or z direction, respectively as shown in Figure 9, the phase velocity will be:

$$V_H = \sqrt{G_{xz}/\rho}$$
$$V_V = \sqrt{G_{zy}/\rho}$$

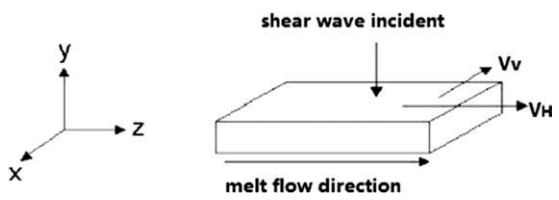

Figure 9 Schematic diagram of incident shear wave propagation in anisotropic media.

where G_{xz} and G_{zy} represent the shear stiffness measured in the x,z and z,y planes, respectively. ρ is the polymer density. The wave equation as above produces two means: a slow velocity for waves with particle displacement vectors pointing in the "weaker" mechanical direction and a fast velocity when the particle velocity vector is in the "strong" direction. Hence, larger difference in echo time corresponds to higher storage modulus.

The time differences between t_V and t_H and during solidification in IM are listed in Table III under different injection conditions by real-time ultrasonic diagnosis. As mentioned above, t_V and t_V demonstrate the time delay of parallel and vertical to the melt flow direction in HDPE, respectively. As summarized in Table III we can see that t_H is larger than t_V, that is to say, the time delay in parallel to the melt flow direction of shear wave is longer than that of vertical direction. The time difference Δt is obtained from the property distinctness of HDPE products. Under the same injection speed, the data in Table III also tell us that the time difference Δt is 0.553 μs in 220°C, which is less than that of 0.656 μs in 210°C. In other words, the particle displacement vector under low temperature is stronger than that in higher temperature, because high temperature helps to disorientate polymer chains. Under the same injection temperature of 220°C, the time difference Δt is 0.553 μs in 60 mm/s injection speed, which is less than that of 0.736 μs in 90 mm/s. Hence, the ultrasonic propagation velocities have greater distinctions between parallel and vertical to melt flow under higher injection speed in IM.

To verify the results of dynamic parameters of HDPE in different injection conditions, offline shear ultrasonic wave is applied on the same samples and same characteristic directions as real-time diagnosis, and the measured results are summarized as in Table IV. As it is summarized in Table IV, Δt at different conditions has the same change tendency as dynamic diagnosis. But the values become smaller than in dynamic measurements because of solidification and relaxation after pressure is released.

The results of dynamic and static ultrasonic diagnosis present that the storage modulus along vertical to the melt flow direction is larger than that along parallel direction. For the sake of validating the

TABLE IV
Offline Shear Wave Parameters of HDPE in Different Injection Conditions

Injection conditions	Thickness (mm)	t_H (μs)	t_V (μs)	Δt (μs)
210°C (60 mm/s)	0.8742	2.02	1.91	0.11
220°C (60 mm/s)	0.836	1.99	1.90	0.09
220°C (90 mm/s)	0.8672	1.99	1.86	0.13

results mentioned above, the tested samples are intercepted and the dynamic mechanical analysis is applied to test the modulus along vertical and parallel to the melt flow directions. As it is shown in Figure 10, the storage modulus along the vertical is larger than that of the parallel to the melt flow direction, which is consistent to the results of ultrasonic diagnosis. But the reason should be studied further.

SEM measurement is also performed to understand the relationship between morphology and properties of storage modulus and ultrasonic propagation. It should be pointed out here that the skin of the sample is cut away using ultrathin section method before etching the amorphous phase of subsurface and the crystalline phase is remained. Figure 11 shows the SEM images of the sample which is prepared under the injection speed of 60 mm/s in 220°C. Figure 11(a shows the image which is magnified by 1000 times and Figure 11(b) is magnified by 2000 times. As shown in Figure 11(a), the trace of melt flow direction can be seen clearly. When the circled part in Figure 11(a) is enlarged, it is distinct that the crystalline lamellas of HDPE are parallel arrangement and grows in a vertical to melt flow direction because injection shear force induces crystallization under a certain injection pressure.[25] As ultrasound propagates faster along crystalline lamellar direction than in melt flow one in polymer, ultrasound can travel faster in vertical direction than that of parallel one in injection mold under our set condition as the results of SEM and DMA presented. Therefore, ultrasound can real-time diagnose polymer storage modulus and morphology indirectly.

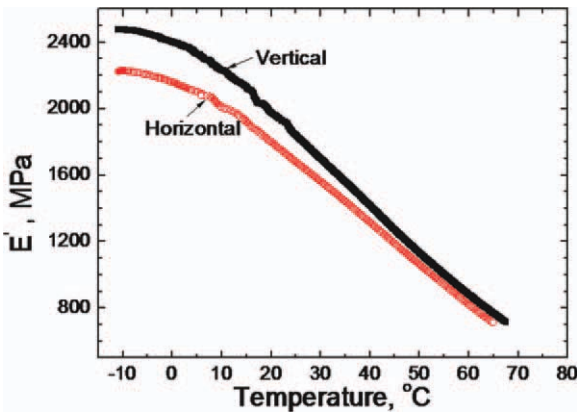

Figure 10 DMA for HDPE samples in vertical and parallel directions. [Color figure can be viewed in the online issue, which is available at wileyonlinelibrary.com.]

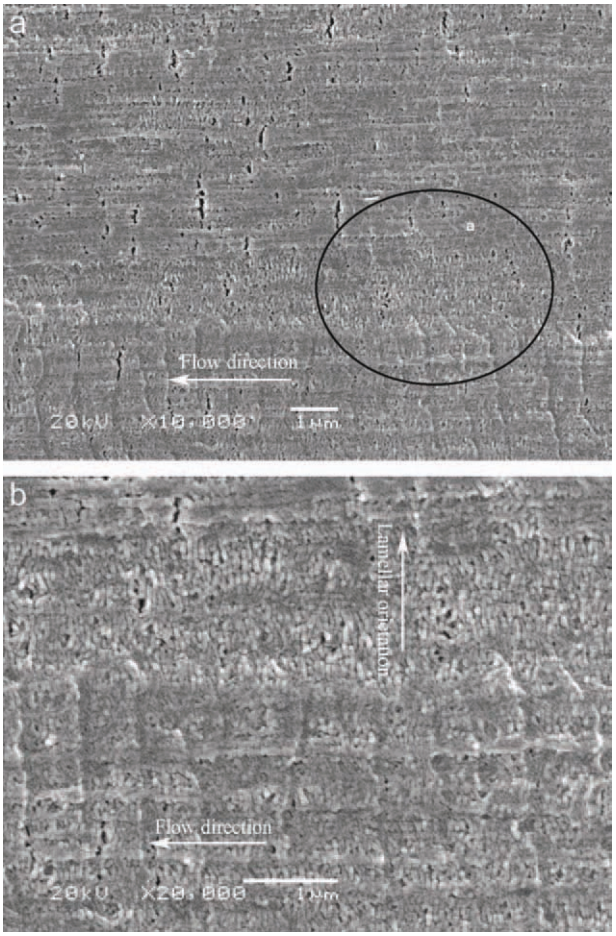

Figure 11 Microface morphology for HDPE sample (a) 10,000× and (b) 20,000×.

CONCLUSIONS

A new real-time ultrasonic diagnosing technique with an L–$S_{\perp}$–$S_{||}$ probe has been integrated onto a mode insert of 150-ton Engel IM machine and real-time noninvasive ultrasonic monitoring combing with IM process has been carried out as well. Real-time diagnosis not only provides the results of the polymer melt flow process, filling and packing stage, solidification process, but also gives us the information about polymer morphology changes and mechanical properties. In this research, we also find an interesting phenomenon that the storage modulus along the vertical is larger than that of the parallel to the melt flow direction under our setup injection conditions because of the crystalline lamella orientations. The investigations in this study help us to study the relationship between the ultrasonic signals and the polymer morphology changes during injection. However, there is still a lot of work should be

developed in future, which can promote ultrasound applications in industrial in a large scale.

References

1. Chen, Z. B.; Turng, L. Adv Polym Tech 2005, 24, 165.
2. Rosato, D. V.; Rosato, D. V. Injection Molding Handbook: The Complete Molding Operation Technology, Performance, Economics; Chapman & Hall: New York, 1995.
3. Kantz, M. R.; Newman H. D. Jr.; Stigale, F. H. J Appl Polym Sci 1972, 16, 1249.
4. Jiang, G. J.; Wu, H.; Yan, B. W.; Guo, S. Y.; Polym Eng Sci 2010, 50, 719.
5. Sunzanne, L. B.; Woll, D. J. C. Polym Eng Sci 1996, 36, 1477.
6. Collins, C. Assembly Automation 1999, 19, 197.
7. Sheth, H. R.; Nunn, R. E. J Injection Molding Technol 2001, 5, 141.
8. Ohta, T.; Yokoi, H. Polym Eng Sci 2001, 41, 806.
9. Brown, E. C.; Mulvaney-Johnson, L.Coates, P. D. Polym Eng Sci 2007, 47, 1730.
10. Gao, F.; Patterson, W. I.; Kamal, M. R. Adv Polym Technol 1994, 13, 111.
11. Kazmer, D.; Barkan, P. Polym Eng Sci 1997, 37, 1880.
12. Piche, L.; Massines, F.; Hamel, A.; Neron, C. US Patent 4754645.
13. Sun, Z.; Yan, J.; Jen, C.-K.; Chen, M.-Y. Polym Eng Sci 2005, 45, 764.
14. Brown, C. E.; Olley, P.; Coates, D. P. Plast Rubber Composites 2000, 29, 3.
15. Cheng, C.-C.; Ono, Y.; Jen, C.-K. Polym Eng Sci 2007, 47, 1491.
16. Brown, E.C.; Olley, P.; Coates, P. D. Processing SPE ANTEC 1997, 1042.
17. Edwards, R.; Thomas, C. Polym Eng Sci 2001, 41, 1644.
18. He, B. B.; Zhang, X. Q.; Zhang, Q.; Fu. Q. J Appl Polym Sci 2008, 107, 94.
19. Moreau, A.; Levesque, D.; Lord, M.; Dubois, M.; Monchalin, J.-P.; Padioleau, C.; Bussiere, J.F. Ultrasonics 2008, 40, 1047.
20. Allen, D. R.; Sayers, C. M. Ultrasonics 1984, 22, 179.
21. King, R. B.; Fortuko, C. M. J Appl Phys 1983, 54, 3027.
22. Kobayashi, M.; Jen, C.-K. Smart Mater Struct 2004, 13, 951.
23. Barrow, D.; Petroff, T. E.; Tandon, R. P.; Sayer, M. J Apply Phys 1997, 81, 876.
24. Wen, S.-S. L.; Jen C.-K.; Nguyen, K.T. Int Polym Process 1999, XIV, 175.
25. Moy, F. H.; Kamal, M. R. Polym Eng Sci 1980, 20, 957.